NASA
Technical Memorandum 4201

AVSCOM
Technical Memorandum 90-B-015

424493

Aerodynamic Performance of a 0.27-Scale Model of an AH-64 Helicopter With Baseline and Alternate Rotor Blade Sets

Accession For
NTIS GRA&I ☒
DTIC TAB ☐
Unannounced ☐
Justification
By
Distribution/
Availability Codes
Dist | Avail and/or Special
A-1

Henry L. Kelley
Aerostructures Directorate
USAARTA-AVSCOM
Langley Research Center
Hampton, Virginia

NASA
National Aeronautics and Space Administration
Office of Management
Scientific and Technical Information Division
1990

QUALITY INSPECTED 4

DISTRIBUTION STATEMENT A
Approved for public release;
Distribution Unlimited

90 07 31 025

Summary

As part of an ongoing research program to improve the aerodynamic efficiency of rotors, the U.S. Army Aerostructures Directorate (ASTD) conducted a rotor performance investigation in the Langley 14- by 22-Foot Subsonic Tunnel using a 0.27-scale model of the AH-64 Apache attack helicopter rotor and fuselage. Two sets of rotor blades were utilized and included baseline blades modeled after the current operational rotor and a set of alternate blades with advanced-design airfoil sections and tapered planform. The purposes of the investigation were to provide experimental validation for the rotor design procedures for the alternate blades and to provide a data base for evaluation of current and future rotor systems for the AH-64.

Aerodynamic forces and moments of the rotor and body were measured both in hover and at forward speeds from 50 knots to 130 knots. Rotor thrust coefficient in hover was varied incrementally from 0.001 to 0.0076 both in and out of ground effect and at tip Mach numbers of 0.64, 0.58, and 0.51.

The results indicated that the design of the alternate rotor was validated in terms of power savings over most of the range of thrust and forward speeds investigated. In hover, at a rotor thrust coefficient of 0.0064, about 6.4 percent less power was required for the alternate rotor than for the baseline rotor. The corresponding thrust increase at this representative hover power condition was approximately 4.5 percent, which represents an equivalent full-scale increase in lift capability of about 660 lb. In forward flight, the improvement in torque required for the alternate rotor was 5 percent to 9 percent at advance ratios μ of 0.15 and 0.20. At the highest speed tested ($\mu = 0.30$), the alternate rotor had a disadvantage in rotor torque of 1.5 percent to 2.5 percent less torque than the baseline rotor. The deficiency in performance is probably caused by the effects of Reynolds number and by differences in elastic properties at the narrow chord blade tips.

Introduction

Research efforts are being pursued within the government and industry to increase overall helicopter efficiency and help meet increasing demands for speed, maneuverability, payload, and range. Efficiency of the main rotor is one area in which significant improvement has been achieved (refs. 1 to 7). Improvements resulting from better airfoils, planform variations, and twist are incorporated into many rotors used on helicopters today. These advanced designs are the results, in part, of the design and fabrication flexibility and cost effectiveness of composite materials.

As part of an ongoing research program to improve the aerodynamic efficiency of rotors, a rotor performance investigation was conducted in the Langley 14- by 22-Foot Subsonic Tunnel using a 0.27-scale model of the AH-64 attack helicopter rotor and fuselage. Two sets of rotor blades were utilized and included baseline blades modeled after the current AH-64 Apache rotor and alternate blades designed by the Aerostructures Directorate (ASTD) at Langley. The alternate blades were designed to improve performance through the use of new airfoils, derived from airfoil research, and planform taper and twist distributions determined from rotor design procedures developed by ASTD engineers at Langley (ref. 1).

The purpose of this investigation was to provide experimental validation of the aforementioned design procedures and to provide a data base for evaluation of current and future rotor systems for the AH-64. Comparison testing between the baseline and alternate configurations and correlation of baseline data with flight data gave added confidence in measured rotor performance differences between the two rotor systems. A similar investigation (refs. 2 and 3) compared a baseline rotor with another ASTD-designed rotor for the UH-1 helicopter and was the initial validation of these design procedures.

In the present investigation, rotor and body forces and moments were measured in hover and at speeds from 50 knots to 130 knots. In hover, rotor thrust coefficient C_T was varied incrementally from 0.001 to 0.0076 both in and out of ground effect (IGE and OGE) and at rotor tip Mach numbers M_{tip} of 0.64, 0.58, and 0.51. Performance in forward flight was obtained from thrust sweeps at three forward speeds. Rotor shaft angle of attack α_s was varied at each advance ratio μ to cover a range of rotor propulsive forces.

The hover results are compared and discussed in terms of rotor torque coefficient C_Q and rotor figure of merit FM as a function of C_T. The forward-flight results are given in terms of rotor lift, drag and torque coefficients, and lift-drag ratio $(L/D)_e$. The effects of M_{tip} and ground proximity on hover performance are presented and discussed. Fuselage download as a function of rotor thrust for both rotors is presented and discussed and comparisons of model rotor data with predicted and full-scale flight results are made. Reynolds number effects on the performance of the alternate rotor are also discussed.

Symbols

Data in this report are presented in coefficient form and are referenced to the shaft-axis system shown in figure 1.

C_D	rotor drag coefficient, $D/\rho\pi R^2(\Omega R)^2$
C_L	rotor lift coefficient, $L/\rho\pi R^2(\Omega R)^2$
C_Q	rotor torque coefficient, $Q/\rho\pi R^3(\Omega R)^2$
C_T	rotor thrust coefficient, $T/\rho\pi R^2(\Omega R)^2$
c	blade chord, ft
c_e	thrust-weighted equivalent blade chord, $\frac{\int_0^1 c(r/R)^2 d(r/R)}{\int_0^1 (r/R)^2 d(r/R)}$, ft
D	rotor drag force, lb
d	rotor diameter, 12.96 ft
FM	figure of merit, $0.707\ \frac{C_T^{3/2}}{C_Q}$
f	equivalent flat-plate drag area, ft^2
H	height from centerline of rotor hub to floor, ft
IGE	in-ground effect
L	rotor lift force, lb
$(L/D)_e$	equivalent lift-drag ratio, $\frac{C_L}{\frac{C_Q}{\mu} - C_D}$
M_{tip}	tip Mach number for rotor advancing blade
N_{Re}	Reynolds number, Vc/ν
OGE	out-of-ground effect
Q	rotor torque, ft-lb
R	rotor radius, 6.48 ft
r	local radius, ft
SLS	sea-level standard atmospheric density conditions at 59°F
T	thrust, lbf
V	free-stream velocity, ft/sec
x, y, z	Cartesian coordinates
Y	rotor side force, lbf
α_s	angle of attack of rotor shaft, deg
α_{TPP}	angle between rotor disk and free-stream velocity (positive nose-up), deg
μ	advance ratio, $V/\Omega R$
ν	kinematic viscosity of air, 1.58×10^{-4} ft^2/sec
ρ	local density of air, slugs/ft^3
σ_T	thrust-weighted solidity, $4c_e/\pi R$
Ω	rotor angular velocity, rad/sec

Apparatus and Procedure

The investigation was conducted in the Langley 14- by 22-Foot Subsonic Tunnel. The experimental hardware included (1) the general rotor model system (GRMS) of the Langley Research Center, (2) a 0.27-scale rotor hub dynamically scaled from the AH-64 hub, (3) a set of 0.27-scale baseline rotor blades scaled geometrically and dynamically from the AH-64 main rotor blade, (4) a set of 0.27-scale ASTD-designed (alternate) rotor blades that were designed to be as dynamically similar to the baseline blades as possible, and (5) a 0.27-scale model fuselage scaled from the AH-64. Pertinent details of the test facility, model hardware, and rotor design considerations are contained in the sections that follow.

Tunnel Description

The Langley 14- by 22-Foot Subsonic Tunnel is a closed-circuit, single-return, atmospheric wind tunnel with a test section that is 14.5 ft high, 21.75 ft wide, and 50.0 ft long. The wind speed is variable from 0 to 200 knots and can be operated in a variety of configurations—closed, slotted, partially open, and open. In the partially open test-section configuration, the floor remains in place and the tunnel is open only on the sides and top. During the present investigation, the open test section was used for hover testing. The floor was lowered 6.75 ft to obtain ground clearance for the OGE ($H/d = 1.4$) portion of the test. Figure 2 is a plan view of a portion of the floor area that was lowered during hover testing relative to the rotor disk area. For forward flight,

data were obtained with the test section closed. A further description of the tunnel is available in reference 8.

The model was supported by a three-joint sting. This sting allowed pitch and yaw positioning to as much as ±45° about a fixed point in the model, so that the rotor remained on the tunnel test-section centerline. The sting was mounted on a model support system that allowed height variation ($0.43 < H/d < 0.87$) with the floor in place as well as some additional pitch and yaw control. For the forward-flight tests, the rotor center of rotation was positioned on the tunnel centerline, 0.56 rotor diameter above the floor.

The tunnel data-acquisition system recorded tunnel operating conditions, atmospheric conditions, and model parameter measurements. The data reduction procedure included corrections for wind-tunnel wall effects that adjusted the tunnel dynamic pressure and flow angularity by the method described in reference 9.

Rotor System

The general rotor model system (GRMS) of the Langley Research Center is a fully instrumented rotor-drive system which can be configured for a wide variety of rotors (refs. 10 to 11) and consists of two 90-hp electric motors, a transmission, and cyclic and collective controls. A maximum usable horsepower of about 160 was available during this test as a result of transmission gearing considerations. The rotor and power train are mounted and suspended within the GRMS on a gimbal that includes pitch and roll springs and adjustable dampers. Figure 3 is a sketch of the AH-64 model mounted on the GRMS, and figure 4 is a photograph of the model attached to the GRMS and installed in the tunnel.

Two six-component, strain-gage balances were used for this test. One supported the fuselage shell, and the other supported the rotor system, including the actuators, electric-drive motors, and transmission. Based on balance design specifications, the rotor balance data are accurate to ±0.000003 for C_Q and ±0.00002 for C_T and represent 0.5 percent of full-balance load. However, previous testing has demonstrated an accuracy of 0.2 percent of full-scale balance load. The fuselage balance had the same accuracy level. The effects of deadweight tares were removed in all cases, and the aerodynamic hub-drag tare was removed prior to the computations of $(L/D)_e$. Rotor rotational speed and rotor azimuthal position were measured by an optical tachometer and trigger. Blade flapping, feathering, and control angles were monitored and recorded. Ten channels of blade strains and one channel of pitch-link strain were also monitored and recorded.

Rotor Hub

The model hub (fig. 5) was dynamically scaled and has the pertinent features of the full-scale hub. A detailed description of the design and development of the hub is presented in reference 12. The hub is fully articulated and features the multilayered strap retention system and elastomeric lead-lag dampers on either side of the pitch cases; these features are unique to the full-scale hub. The pitch case encloses the straps and transmits the feathering input to the blade. As with the full-scale hub, the lead-lag motion of the blade takes place through a fitting that connects to the outboard end of the pitch case, the blade, and the lead-lag dampers.

Blades

Figure 6 is a plan view that shows key parameters of the model blades. The baseline blade had a linear twist of −9°, a 10.5-percent-thick cambered Hughes Helicopters (HH-02) airfoil from the root to the 0.943 blade radius station, and a 20°-swept tip that included a linear transition to an NACA 64A006 airfoil at the blade tip. The alternate blade had a linear twist of −12°, an increased inboard chord of 7.17 in., and a 5-to-1 planform taper from the 0.8 blade radius station to the tip. Both rotors had a thrust-weighted solidity of 0.0928. Three airfoil sections developed at the ASTD for rotorcraft application were utilized on the alternate rotor. The RC(3)-08 and RC(3)-10 airfoils are described in reference 13. The data that describe the modified RC(3)-10 airfoil are unpublished.

The blades were fabricated from composite materials to meet the demanding requirements of dynamic similarity and Mach number scaling. Details of the design and development of the baseline blades are available in reference 12. The alternate blades were designed and developed using similar methods and materials. Typical materials included foam, balsa, nomex honeycomb, fiberglass, S glass, Du Pont Kevlar, graphite fiber, epoxy, and tungsten balance weights.

The accuracy of the contours of both blade sets was held to 0.005 in. or less. Strain gages were installed in depressions on the blades; these depressions were then filled and smoothed. Wires were run inside conduit that was molded into the blades to help maintain a smooth outer surface.

Blade specimens were fabricated and evaluated to obtain correctly scaled mass, stiffness, inertia, and balance properties. Root specimens for both blade

sets were tested to failure to establish structural integrity.

The baseline blade structural and dynamic properties are presented in reference 12. An effort was made to preserve the full-scale dynamic properties in both sets of model blades, but there were difficulties in the tip region with the alternate blades. The taper at the tip, in conjunction with the model scale, resulted in dimensions in the tip region that yielded insufficient volume to accurately model mass and stiffness characteristics. The model rotor blade weight as a function of blade radius is presented in figure 7 for the baseline, alternate, and full-scale blades. The data in the figure that were scaled to match full scale were taken from the manufacturer.

The predicted performance for the alternate blade design was about 7 percent better than for the baseline configuration in power required for hover and 2 to 9 percent better in power required for forward flight (fig. 8). The prediction method for hover performance was a Langley-developed momentum blade-element analysis, and the forward-flight prediction method used was C81 (ref. 14).

Fuselage

The fuselage was scaled from the flight configuration except for the tail boom, which required a constant diameter large enough to accommodate the sting (fig. 3). Because of fouling problems between the sting and tail boom during the test, the portion of the fuselage from the tail boom juncture rearward was not metric (connected to a strain-gage balance) as indicated in figure 3. The horizontal and vertical tails were not utilized during this test. All configurations included 16 wing-mounted model missiles, except during a portion of the rotor-off tests. The fuselage shell and tail boom were made from fiberglass-epoxy material. The wings, pylons, missile racks, missiles, horizontal and vertical stabilizer, and landing gear were machined from wood and metal.

Test Procedures

Tests were conducted in hover and at forward speeds for both sets of blades. Hover testing was conducted in and out of ground effect; the rotor shaft was vertical and resulted in a 5° nose-up fuselage angle. Forward-speed tests were conducted from 50 to 130 knots for both rotor sets.

In hover, performance data were taken with values of H/d from 0.43 to 1.4 to investigate the effects of ground proximity on performance. The model support structure prevented testing to $H/d \approx 0.30$ with the wheels on the ground. As discussed previously, the wind-tunnel test-section walls and ceiling were raised, and the floor was lowered when testing in hover for the out-of-ground-effect conditions and resulted in $H/d = 1.4$. The performance of both rotors was evaluated at rotor blade tip Mach numbers of 0.64, 0.58, and 0.51. These tip speeds represented model rotor rpm's of 1070, 963, and 856, respectively.

Ground-effect data for hover, including fuselage download, were obtained with the wind-tunnel test section in the partially open configuration (sidewalls and ceiling raised and floor in place). Beginning with the floor in place and the model at the maximum height permitted by the support system ($H/d = 0.87$), power was maintained at a constant torque coefficient setting ($C_Q \approx 0.00048$), and the model was lowered in increments until the lowest height permitted by the support system was reached ($H/d = 0.43$).

At forward speeds, better flow quality in the test section was maintained by testing in the closed test-section configuration. A value of H/d of 0.56 was maintained; this value placed the rotor disk at the tunnel vertical centerline. An analysis of corrections due to wall effects indicated that this height resulted in minimum wall and support-system flow interference. Rotor lift variations were made at advanced ratios μ of 0.15, 0.20, and 0.30. At each value of μ, three angles of attack α_s were tested to provide a variation in rotor propulsive force. Rotor lateral and longitudinal flapping with respect to the shaft were maintained at 0° to reduce rotor hub vibratory loads. The data were analyzed and plotted in terms of rotor drag coefficient versus torque coefficient at constant levels of rotor lift. Also, the data were analyzed in terms of rotor $(L/D)_r$ as a function of both rotor C_T and μ.

Since the model hardware was new and unproven under operating conditions in the tunnel, a conservative test matrix was selected. The thrust and speed conditions tested were below the thrust and speed capability of the full-scale AH-64. Examination of flight data showed that forward speeds to about 200 knots (diving flight) and rotor thrust coefficients to 0.0092 (hover; OGE) were reached by the AH-64.

Presentation of Results

The data are presented as outlined in the table below:

Figure	Parameters	μ	Hover M_{tip}	H/d	Comparison
9	C_Q vs C_T	Hover	0.64	1.4	Baseline vs alternate
10	FM vs C_T	Hover	.64		Baseline vs alternate
11	C_Q vs C_T	Hover	.58		Baseline vs alternate
12	FM vs C_T	Hover	.58		Baseline vs alternate
13	C_Q vs C_T	Hover	.51		Baseline vs alternate
14	FM vs C_T	Hover	.51		Baseline vs alternate
15	Fuselage download vs rotor thrust	Hover	.64		Baseline vs alternate
16	C_T vs H/d	Hover		Varied	Baseline vs alternate
17	C_D/σ_T vs C_Q/σ_T	0.15 to 0.30		0.56	Baseline vs alternate
18	$(L/D)_e$ vs C_T/σ_T	0.15 to 0.30		.56	Baseline vs alternate
19	Vehicle torque coefficient vs C_T	Hover		1.4	Baseline vs full scale
20	Vehicle torque coefficient vs forward speed	0.12 to 0.35			Baseline vs full scale

Results and Discussion

Hover

The hover performance results for the baseline and alternate rotors are compared in terms of C_Q versus C_T and FM versus C_T at $M_{tip} = 0.64$ (100 percent rpm) in figures 9 and 10, respectively. The alternate rotor required a lower C_Q (less power required) for a given value of C_T in the range above 0.002 (fig. 9). The sea-level-standard (SLS) thrust condition C_T for the full-scale helicopter at a normal operational weight of 14 667 lb is 0.0064. As seen in the figure, for that thrust condition, about 6.4 percent less power was needed for the alternate rotor than for the baseline rotor. The thrust increase at $C_Q \approx 0.00049$, corresponding to the aircraft weight of 14 667 lb, was approximately 4.5 percent, which represents an increase in lift capability of about 660 lb at that vehicle weight. Specifically, the advantage in C_Q for the alternate rotor as measured from figure 9 was 5.7 percent, 6.2 percent, 5.1 percent, and 3.7 percent at $C_T = 0.0050$, 0.0060, 0.0070, and 0.0073, respectively. A value of $C_T = 0.0080$ corresponds to a full-scale weight of 14 667 lb at 4000 ft and 95°F and was close to the highest thrust tested at $M_{tip} = 0.64$ for the alternate rotor. The 4000-ft, 95°F condition is an important design criterion for Army helicopters to ensure adequate operational performance under hot-day, high-altitude conditions.

As seen in figure 10, the improvement in FM for the alternate rotor was reduced from 6.4 percent at SLS to 5.4 percent at $C_T = 0.0073$, which is near the peak FM tested for the baseline rotor. The calculated design goal of a 7-percent improvement in hover power required (fig. 7) for the alternate rotor was nearly met.

Effects of Tip Mach Number

Hover performance data obtained by using identical test techniques at $M_{tip} = 0.58$ (90 percent rpm) and 0.51 (80 percent rpm) are given in figures 11 to 14. Examination of these data in conjunction with the data of figures 9 and 10 ($M_{tip} = 0.64$) revealed two trends worthy of note as rotor tip Mach number was reduced. First, the performance improvement for the alternate rotor in terms of FM at $C_T = 0.0064$ is reduced from 6.4 percent at $M_T = 0.64$ to 2.8 percent at $M_{tip} = 0.51$ (compare figs. 10 and 14). Second, both rotors achieved higher values of FM at reduced M_{tip}. The peak value of FM for the alternate rotor was 0.80, 0.79, and 0.78 at $M_{tip} = 0.51$, 0.58, and 0.64, respectively. Also, a crossover in the performance curves at the lower thrust coefficients occurred below a usable flight operational level. For example, at $M_{tip} = 0.51$ (fig. 14), the curves cross at $C_T \approx 0.0047$. Similar trends have been observed and reported in references 15 and 16. Specifically, the increase in FM with reduced M_{tip} and the crossover of FM at low values of C_T with reduced M_{tip} agree with results reported in reference 15.

The reduced performance between the alternate and baseline blades as a function of M_{tip} are not completely understood at present, but the effect of N_{Re} is likely to be one of the factors. For example, the advanced rotor had a blade tip chord of 1.43 in. and a hover tip speed of 727 ft/sec; these factors resulted in a tip Reynolds number of about 0.5×10^6. Large changes in aerodynamic characteristics are known to occur in this range. By comparison, the tip Reynolds number for the model baseline blade in hover is about 2.2×10^6 at a rotor tip speed of 727 ft/sec. Similar results were observed in a model rotor test (ref. 16) with rotor blades that had a 5:1 planform tip taper. Another factor that has perhaps an even larger effect on rotor aerodynamic performance is blade elastic properties (ref. 17). One conclusion in reference 17 indicated that N_{Re} effects may be minor in rotor aerodynamic testing compared with the effect of blade elastic properties (dynamically scaled rotor blades versus "rigid" blades).

Fuselage Download

Accurate prediction of hover performance loss due to fuselage download is still a difficult design problem. The measured fuselage download for both rotors at $H/d = 1.4$ and at $M_{tip} = 0.64$ is given in figure 15 as a function of rotor thrust. The fuselage configuration included wings and 16 wing-mounted model missiles. A small increase in fuselage download was measured for the alternate blade over a thrust range of 250 to 1250 lb. It was expected that the download from the alternate rotor would be greater than from the baseline, since the alternate design called for increased inboard loading (higher twist; more blade area inboard). At a rotor thrust of 1070 lb ($C_T = 0.0064$), an increase in fuselage download equivalent to about 0.5 percent of the total rotor thrust was measured for the alternate rotor (fig. 15). When this increase in download is subtracted from the thrust gain for the alternate rotor (fig. 9), a net performance gain of 4.0 percent thrust at $C_T = 0.0064$ is realized.

The download measured for the baseline rotor was nominally 5 to 6 percent of rotor thrust for a typical hover thrust condition ($C_T = 0.0064$). Tail-boom download calculations, based on rotor wake velocity, vertical drag coefficient, and tail boom area, indicated that the tail-boom contribution increases download by an additional 0.5 percent. Based on measurements obtained during this investigation and on results from similar investigations (refs. 15 and 18), the download results are reasonable.

Ground Effects

The effect of the ground presence on the hover performance of both rotors is given in figure 16 in terms of C_T versus H/d at $C_Q = 0.00048$ (nominal value). Fuselage download was not subtracted from rotor thrust in these data. The results indicate that ground effect on the performance of both rotors is virtually equal; the largest difference is less than 0.5-percent rotor thrust at $H/d = 0.43$ (wheels about 6 ft above the ground at full scale).

Ground effects on fuselage download were measured and analyzed. As height was reduced from $H/d = 1.4$ to $H/d = 0.43$, there was a reduction in fuselage download (−73 lb) of approximately the same magnitude as the increase in rotor thrust (+65 lb). Approximately one-half of the total positive ground-effect cushion experienced by the model was therefore generated by changes in fuselage vertical force; the remainder of the ground cushion can be attributed to the more familiar rotor thrust cushion. Specifically, the fuselage vertical load with either the baseline rotor or the alternate rotor installed changed from a download at $H/d = 1.4$ to an upload at $H/d = 0.43$. These effects on helicopter fuselage download as a function of height are consistent with previously published results (refs. 15 and 19). Also, the ground effects on the performance of the complete model were in agreement when compared with flight data and calculated results (ref. 20).

Forward Flight

Rotor lift variations. Incremental rotor lift variations for the alternate and baseline rotors were performed (fig. 17) at $\mu = 0.15$ (65 knots), 0.20

(86 knots), and 0.30 (130 knots). The lift variations were made at three values of α_s to vary the rotor drag force at each value of μ. Data were not obtained below $\mu = 0.15$ because of the excessively large tunnel wall corrections that were required. At each value of μ, the results from both rotors are compared in terms of rotor drag coefficient C_D/σ_T versus rotor torque coefficient C_Q/σ_T for three levels of rotor lift coefficient C_L/σ_T. The variation of C_L/σ_T investigated represents a range in full-scale aircraft weight from approximately 10 600 lb to 16 000 lb at SLS atmospheric conditions. Figure 17 shows crossplots of C_L/σ_T versus C_D/σ_T and C_L/σ_T versus C_Q/σ_T. This method permits C_Q/σ_T comparisons between the two rotors to be made at constant values of C_L/σ_T and rotor propulsive force.

At $\mu = 0.15$ (fig. 17(a)), the alternate rotor had a lower required value of C_Q/σ_T than the baseline rotor over the entire range of C_D/σ_T investigated and for each of the three C_L/σ_T conditions. The reduction in C_Q/σ_T required for the alternate rotor was nominally 6 to 8 percent over the entire range of lift and propulsive forces investigated.

At $\mu = 0.20$ (fig. 17(b)), C_Q/σ_T required for the alternate rotor was nominally 5 to 9 percent less than for the baseline rotor over the range of lift and drag investigated. The improvement in C_Q/σ_T for the alternate rotor was 8.7 percent at a $C_L/\sigma_T = 0.073$ and $C_D/\sigma_T = -0.0033$. This level of improvement is approximately the same as that given in the previous discussion for $\mu = 0.15$.

At $\mu = 0.30$ (fig. 17(c)), C_Q/σ_T required for the alternate rotor was 1.5 to 2.5 percent higher than for the baseline rotor over the range of lift and drag investigated. At this value of μ, the calculated design goal for the alternate rotor of a performance advantage of 2 percent compared with the baseline was not met. A portion of the performance disadvantage for the alternate rotor could have been caused by operation at subcritical Reynolds numbers in the rotor tip region. Differences in elastic properties in the blade tip region could have been another contributing factor. The narrow chord tip (1.43 in.), created by both scaling and design (5 to 1 tip taper ratio), resulted in a retreating blade tip with $N_{Re} = 0.373 \times 10^6$ at $\mu = 0.30$. Large subcritical Reynolds number effects could occur at numbers in this range. At $\mu = 0.15$, the Reynolds number at the retreating tip of the alternate rotor was 0.468×10^6. By comparison, the baseline rotor had retreating blade tip Reynolds numbers of 1.48×10^6 and 1.86×10^6 for $\mu = 0.30$ and $\mu = 0.15$, respectively. Airfoil data taken over the range of Reynolds numbers of interest were not available to correct the performance data.

At full scale, these rotors also exhibit large differences in tip Reynolds number, and aerodynamic performance differences would be expected as a result. For example, at an advance ratio of 0.30 (about 130 knots forward speed), the full-scale Reynolds numbers at the retreating blade tip would be about 1.4×10^6 and 5.5×10^6 for the alternate rotor and baseline rotor, respectively. The effects of Reynolds number would be expected to be less, however, in the higher range of Reynolds numbers afforded by the full-scale dimensions.

Rotor cruise efficiency. Rotor cruise efficiency in terms of $(L/D)_e$ was calculated for the two rotors using data obtained during rotor lift variations at $\mu = 0.15$, 0.20, and 0.30 (fig. 18). At each speed, a value of α_s was used that represented a trim propulsive force equal to a full-scale flat-plate drag area of about 34 ft^2. The equation used in the calculation was

$$\left(\frac{L}{D}\right)_e = \frac{C_L}{\frac{C_Q}{\mu} - C_D}$$

A measured value of the rotor hub drag coefficient (0.0001253) was subtracted from the rotor drag term. The lift, drag, and torque values were derived from the rotor balance data. For example, at $C_T/\sigma_T = 0.07$, the alternate rotor indicated improvements in $(L/D)_e$ of 9.3 percent and 10.4 percent at $\mu = 0.15$ and 0.20, respectively (fig. 18). At $\mu = 0.30$ and at the same C_T/σ_T, however, the alternate rotor indicated a 0.3-percent disadvantage in $(L/D)_e$. The decline in performance at $\mu = 0.30$ follows the aforementioned trend (fig. 17(c)), where the alternate rotor displayed a 2.5-percent disadvantage in C_Q/σ_T required. Also, the same reasons for the decline in performance offered in the previous discussion apply in this case. Results obtained at the ASTD on a rotor designed for a modern utility helicopter with similar blade design techniques (3 to 1 tip taper) but without the pitfalls of N_{Re} through the use of Freon 12 as a test medium in the wind tunnel indicated significant performance improvements up to $\mu = 0.37$ and $C_L = 0.0107$ (ref. 21).

The forward-flight rotor performance trends all point to large improvements for the alternate rotor (up to 10 percent) over the speed range investigated except at the $\mu = 0.30$ condition, where a small deficiency occurs for the alternate rotor. Data at full-scale Reynolds number values are needed to get a more accurate indication of relative performance between these kind of rotors at the high-speed, high-lift conditions.

Comparison of Model Data With Flight Data

Comparison of wind-tunnel model data to flight data is of interest as another way to increase confidence in model results. Hover and forward-speed performance results for the baseline rotor are compared with flight data taken on the full-scale AH-64 helicopter in figures 19 and 20, respectively. Flight data used in the comparison were obtained from reference 22.

Hover. Hover out-of-ground-effect data are plotted as vehicle torque coefficient versus thrust coefficient over a range of thrust coefficients from 0.0050 to 0.0083 (fig. 19). The model supplied data for the rotor only, and corrections were then applied for the power consumption of auxiliary hydraulic and electrical devices, gearboxes, tail rotor, and fuselage download. The formula used to correct the model data for these items was supplied by the aircraft manufacturer. The fuselage download correction was measured during this investigation, and these values have been included in the correction. The corrected model data are in good agreement with the flight data, although the model hover performance data had about 2 to 4 percent higher thrust for a given torque coefficient over the range tested. This result is contrary to the experience of past investigations (refs. 4, 15, and 17), which have shown that model rotor performance results are pessimistic. That is, performance is better with full-scale aircraft than with models. Low Reynolds number effects associated with models have been identified as one of the primary factors responsible for the reduced performance. The reason for the opposite trend in the present investigation is probably the correction to the model rotor-alone data to account for losses in tail-rotor power and subsystem power. Also, the model may have experienced beneficial ground effects from the presence of the fuselage and possible tunnel test-section recirculation.

Forward flight. The forward-flight performance results for the baseline rotor are compared with flight data and plotted as vehicle torque coefficient versus forward speed for a full-scale vehicle gross weight of 14 667 lb, a flat-plate drag area f of 33.8 ft^2, and SLS atmospheric conditions in figure 20. The model-to-flight correlation was generally quite good (within usual flight-test accuracy of 5 percent) and provided additional confidence in the model results. The technique for correcting the model data for losses in tail-rotor power and transmission power was taken from figure 5 of reference 19.

Conclusions

Performance of a 27-percent, dynamically scaled model of an alternate rotor designed for the AH-64 Apache attack helicopter mission was measured in hover and at forward speeds between 50 and 130 knots. A baseline rotor, modeled after the current AH-64 rotor, was also investigated to provide comparisons. The purposes of the investigation were to validate procedures used at the Aerostructures Directorate (ASTD) to design rotors with increased performance potential and provide a database against which to evaluate current and future rotor systems. The predicted performance improvement for the alternate blade design was to provide about a 7-percent improvement in power required in hover and a 2- to 9-percent improvement in power required in forward flight over those required for the baseline. Fuselage download and ground effects in hover were also investigated. Model and flight data were compared. Based on analyses of data obtained during this investigation, the following conclusions are drawn:

1. In hover, at a thrust coefficient C_T of 0.0064, the calculated design goal of a 7-percent improvement in power required (alternate rotor versus baseline rotor) was nearly met. Specifically, the improvement in torque coefficient C_Q was 5.7 percent, 6.2 percent, 5.1 percent, and 3.7 percent at a C_T = 0.0050, 0.0060, 0.0070, and 0.0073, respectively. At C_T = 0.0064, which corresponds to a full-scale aircraft weight of 14 667 lb at sea-level-standard (SLS) atmospheric conditions, an increase in thrust capability of 4.5 percent was realized for the alternate rotor. This increase in thrust capability represents an increase in lift capability of about 660 lb at that vehicle weight.

2. In forward flight, the reduction in rotor torque coefficient C_Q/σ_T for the alternate rotor was nominally 6 to 8 percent and 5 to 9 percent at advance ratios μ of 0.15 and 0.20, respectively, for the range of C_L/σ_T and C_D/σ_T investigated. At μ = 0.30, the alternate rotor had a disadvantage in C_Q/σ_T of 1.5 to 2.5 percent over the range of rotor lift coefficient C_L/σ_T and rotor drag coefficient C_D/σ_T investigated. The calculated design goal of a 2-percent performance advantage at μ = 0.30 for the alternate rotor compared with the baseline was not met. The calculated performance advantage for the alternate rotor was met or exceeded for the μ = 0.15 and 0.20 cases.

3. The reduced performance gains for the alternate rotor at high C_T in hover and at an advanced ratio of 0.30 are probably the result of Reynolds number effects and to differences in blade elastic properties, particularly in the tapered tip region. These effects are present at full scale, but would be expected to be less at the higher Reynolds number range afforded at full scale.

4. At a hover out-of-ground-effect condition with $C_T = 0.0064$, the fuselage download for the alternate rotor was higher by about 0.5 percent of the rotor thrust; this difference was probably caused by increased inboard loading designed into the alternate rotor through the use of higher twist and longer inboard chord. When the increase in download is subtracted from the thrust gain for the alternate rotor, the net performance gain is reduced slightly from 4.5 percent to 4.0 percent at $C_T = 0.0064$.

5. Operating at reduced rotor tip Mach numbers ($M_{tip} = 0.58$ and 0.51 compared with $M_{tip} = 0.64$) reduced the hover performance advantage for the alternate rotor in terms of figure of merit at $C_T = 0.0064$ from 6.4 percent at $M_{tip} = 0.64$ to 2.8 percent at $M_{tip} = 0.51$. The reduced performance increments are not completely understood, but the effect of Reynolds number is probably one of the factors.

6. In hover with either rotor, the fuselage vertical force changed from a download at rotor height to rotor diameter ratios H/d between 0.5 and 1.4 to a fuselage upload at H/d between 0.43 and 0.5. In fact, approximately one-half the total ground-cushion benefit from the model came from fuselage upload.

7. The ground had virtually the same effect on hover performance for the two rotors at $0.43 < H/d < 1.4$.

NASA Langley Research Center
Hampton, VA 23665-5225
May 9, 1990

References

1. Bingham, Gene J.: The Aerodynamic Influences of Rotor Blade Airfoils, Twist, Taper and Solidity on Hover and Forward Flight Performance. *Proceedings of the 37th Annual National Forum, American Helicopter Soc., Inc.*, 1981, pp. 37–50.
2. Berry, John D.: Quarter-Scale Testing of an Advanced Rotor System for the UH-1 Helicopter. *37th Annual Forum Proceedings, American Helicopter Soc., Inc.*, 1981, pp. 456–462.
3. Berry, John D.: *Performance Testing of a Main Rotor System for a Utility Helicopter at 1/4 Scale*. NASA TM-83274, AVRADCOM TR 82-B-3, 1982.
4. Keys, Charles N.; McVeigh, Michael A.; Dadone, Leo; and McHugh, Francis J.: Considerations in the Estimation of Full-Scale Rotor Performance From Model Rotor Test Data. *Proceedings of the 39th Annual Forum of the American Helicopter Society*, May 1983, pp. 34–43.
5. Fradenburgh, Evan A.: Aerodynamic Factors Influencing Overall Hover Performance. *Aerodynamics of Rotary Wings*, AGARD-CP-111, Feb. 1973, pp. 7-1–7-11.
6. Amer, Kenneth B.; and Prouty, Raymond W.: Technology Advances in the AH-64 Apache Advanced Attack Helicopter. *39th Annual Forum Proceedings, American Helicopter Soc.*, 1983, pp. 550–568.
7. McVeigh, Michael A.; and McHugh, Francis J.: Influence of Tip Shape, Chord, Blade Number, and Airfoil on Advanced Rotor Performance. *J. American Helicopter Soc.*, vol. 29, no. 4, Oct. 1984, pp. 55–62.
8. Applin, Zachary T.: *Flow Improvements in the Circuit of the Langley 4- by 7-Meter Tunnel*. NASA TM-85662, 1983.
9. Heyson, Harry H.: *Use of Superposition in Digital Computers To Obtain Wind-Tunnel Interference Factors for Arbitrary Configurations, With Particular Reference to V/STOL Models*. NASA TR R-302, 1969.
10. Murrill, Robert J.: *Operation and Maintenance Manual for the General Rotor Model System*. NASA CR-145230, 1977.
11. Wilson, John C.: A General Rotor Model System for Wind-Tunnel Investigations. *J. Amer.*, vol. 14, no. 7, July 1977, pp. 639–643.
12. Straub, F. K.; Johnston, R. A.; Head, R. E.; and Kelley, H. L.: Design and Development of a Dynamically Scaled Model AH-64 Main Rotor. *Tenth European Rotorcraft Forum (The Hague, The Netherlands)*, Aug. 1984, pp. 63-1–63-21.
13. Bingham, Gene J.; and Noonan, Kevin W.: *Two-Dimensional Aerodynamic Characteristics of Three Rotorcraft Airfoils at Mach Numbers From 0.35 to 0.90*. NASA TP-2000, AVRADCOM TR 82-B-2, 1982.
14. Van Gaasbeek, J. R.: *Rotorcraft Flight Simulation, Computer Program C81, Volume II—User's Manual*. USARTL-TR-77-54B, U.S. Army, Oct. 1979. (Available from DTIC as AD A079 632.)
15. Balch, David T.: Experimental Study of Main Rotor/Tail Rotor/Airframe Interaction in Hover. *39th Annual Forum Proceedings, American Helicopter Soc.*, 1983, pp. 1–14.
16. Phelps, Arthur E., III; and Althoff, Susan L.: *Effects of Planform Geometry on Hover Performance of a 2-Meter-Diameter Model of a Four-Bladed Rotor*. NASA TM-87607, AVSCOM TR 85-B-6, 1986.
17. Yeager, William T., Jr.; and Mantay, Wayne R.: *Correlation of Full-Scale Helicopter Rotor Performance in Air With Model-Scale Freon Data*. NASA TN D-8323, 1976.
18. Flemming, Robert J.; and Erickson, Reuben E.: An Evaluation of Vertical Drag and Ground Effect Using the RSRA Rotor Balance System. *38th Annual Forum Proceedings, American Helicopter Soc.*, 1982, pp. 43–54.
19. Fradenburgh, Evan A.: Aerodynamic Design of the Sikorsky S-76 Helicopter. Preprint No. 78-06, *34th Annual National Forum, American Helicopter Soc., Inc.*, May 1978.
20. Gessow, Alfred; and Myers, Garry C., Jr.: *Aerodynamics of the Helicopter*. Frederick Ungar Publ. Co., c.1952.
21. Yeager, William T., Jr.; Mantay, Wayne R.; Wilbur, Matthew L.; Cramer, Robert G., Jr.; and Singleton, Jeffrey D.: *Wind-Tunnel Evaluation of an Advanced Main-Rotor Blade Design for a Utility-Class Helicopter*. NASA TM-89129, AVSCOM TM-87-B-8, 1987.
22. Bender, Gary L.; Diekmann, Vernon L.; Attomeyer, John D.; Picasso, Bartholomew D., III; and Higgins, Larry B.: Engineering Design Test 4—YAH-64 Advanced Attack Helicopter. USAAEFA Project No. 80-03, U.S. Army, Jan. 1980.

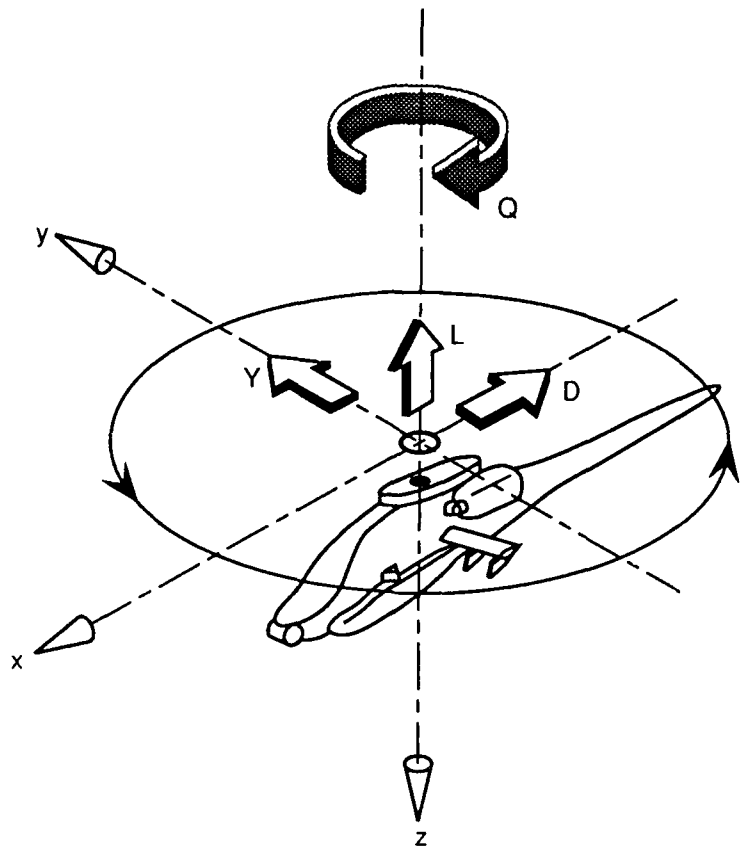

Figure 1. Axis system used for presentation of data. Arrows denote positive directions of forces, moments, and axes.

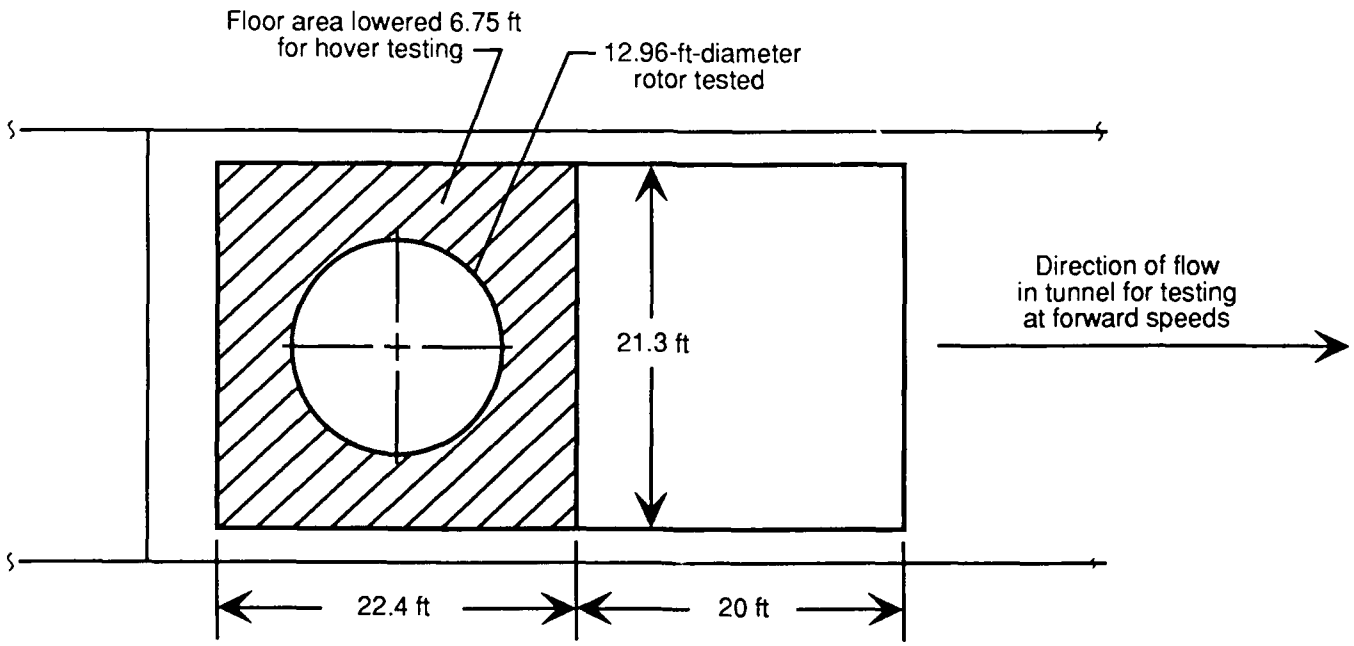

Figure 2. Plan view of test-section floor of Langley 14- by 22-Foot Subsonic Tunnel showing size of rotor area relative to area of floor lowered during hover testing.

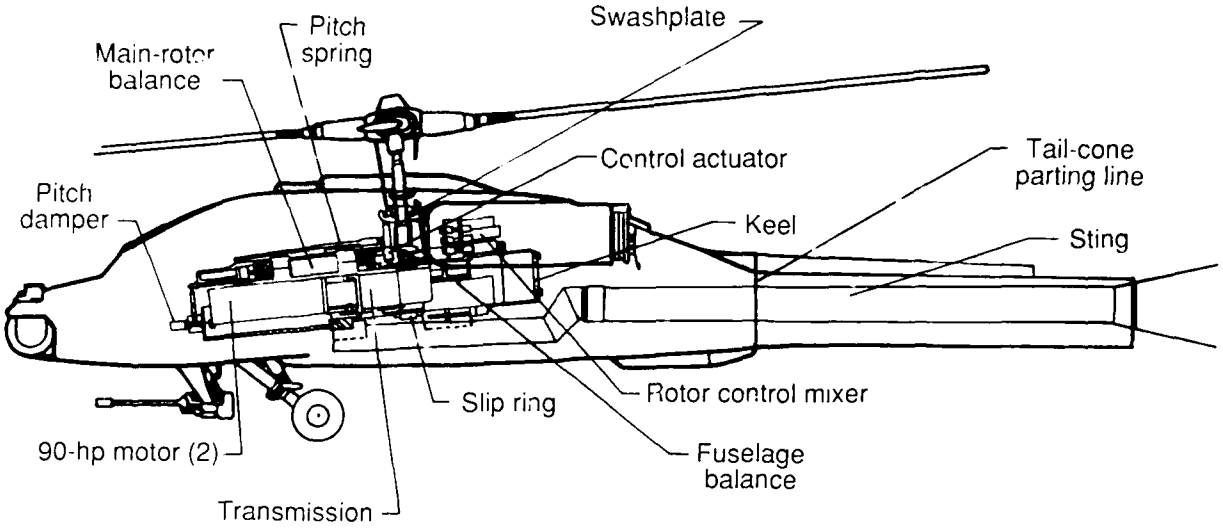

Figure 3. Sketch of AH-64 fuselage model installed on the general rotor model system (GRMS) of the Langley Research Center.

L-84-1825

Figure 4. AH-64 model with alternate blades in Langley 14- by 22-Foot Subsonic Tunnel.

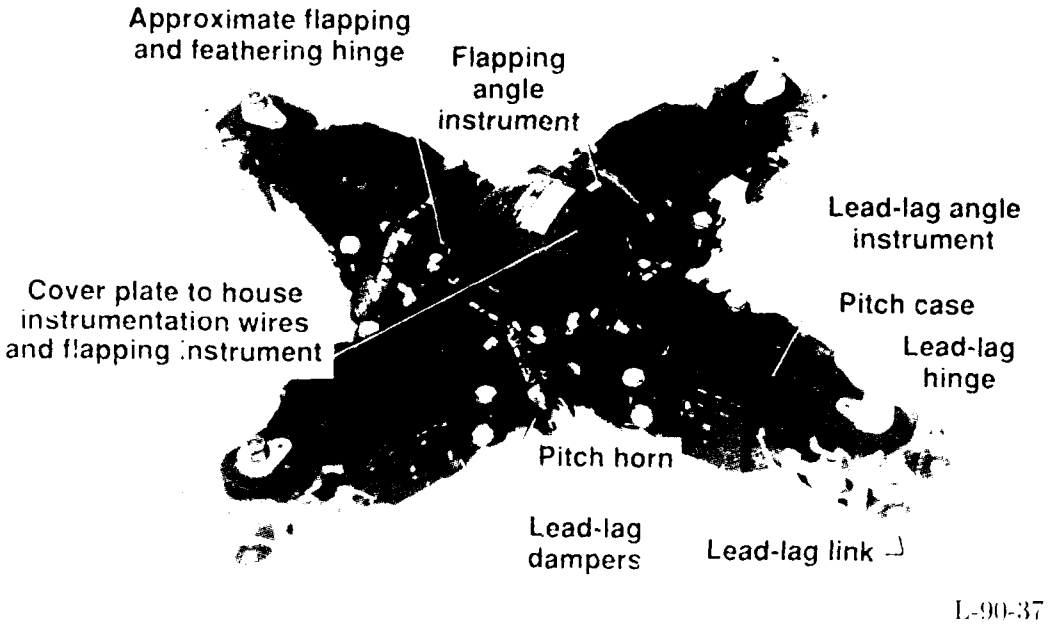

Figure 5. Model hub with some major components indicated.

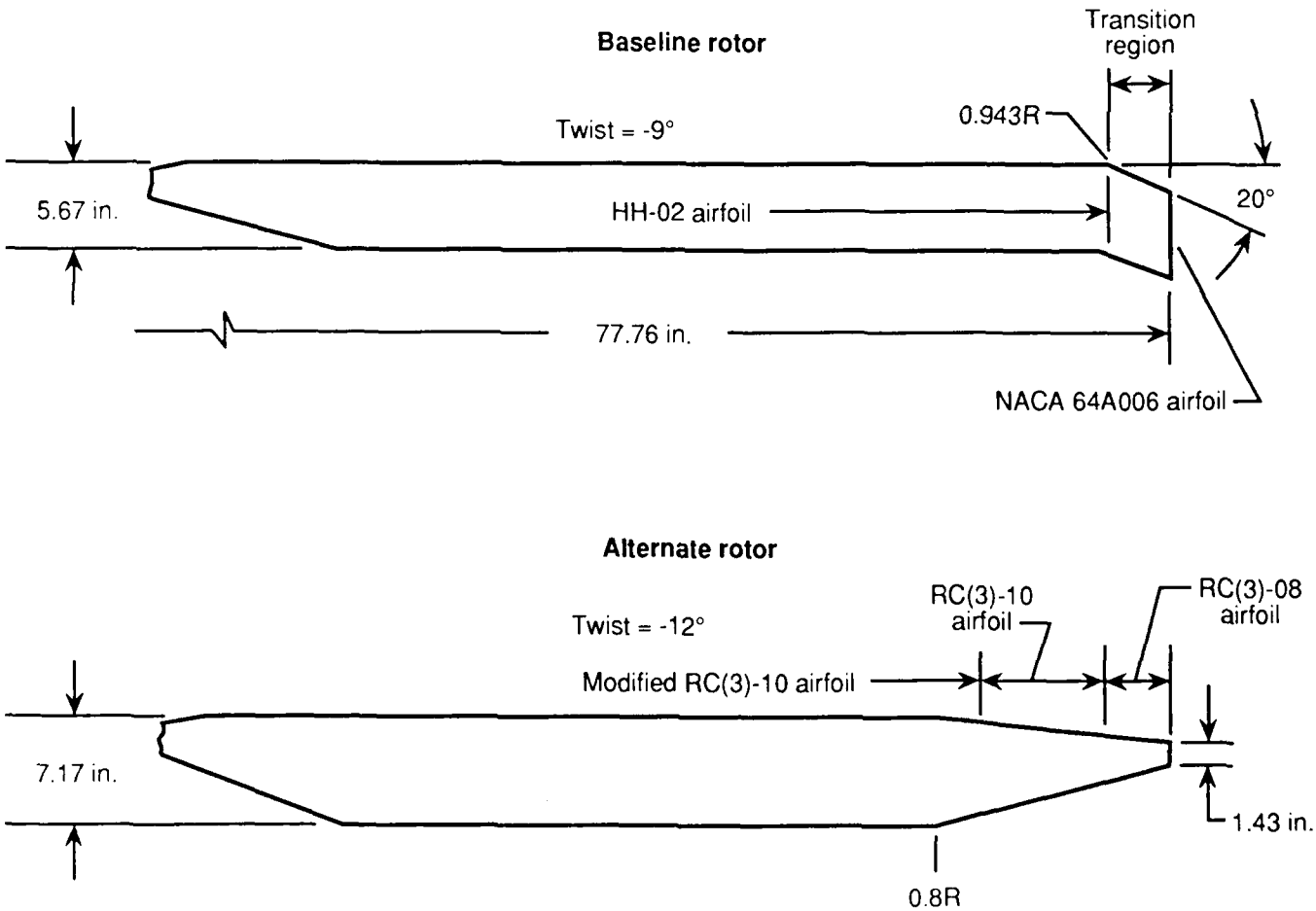

Figure 6. Geometric characteristics of rotor blade.

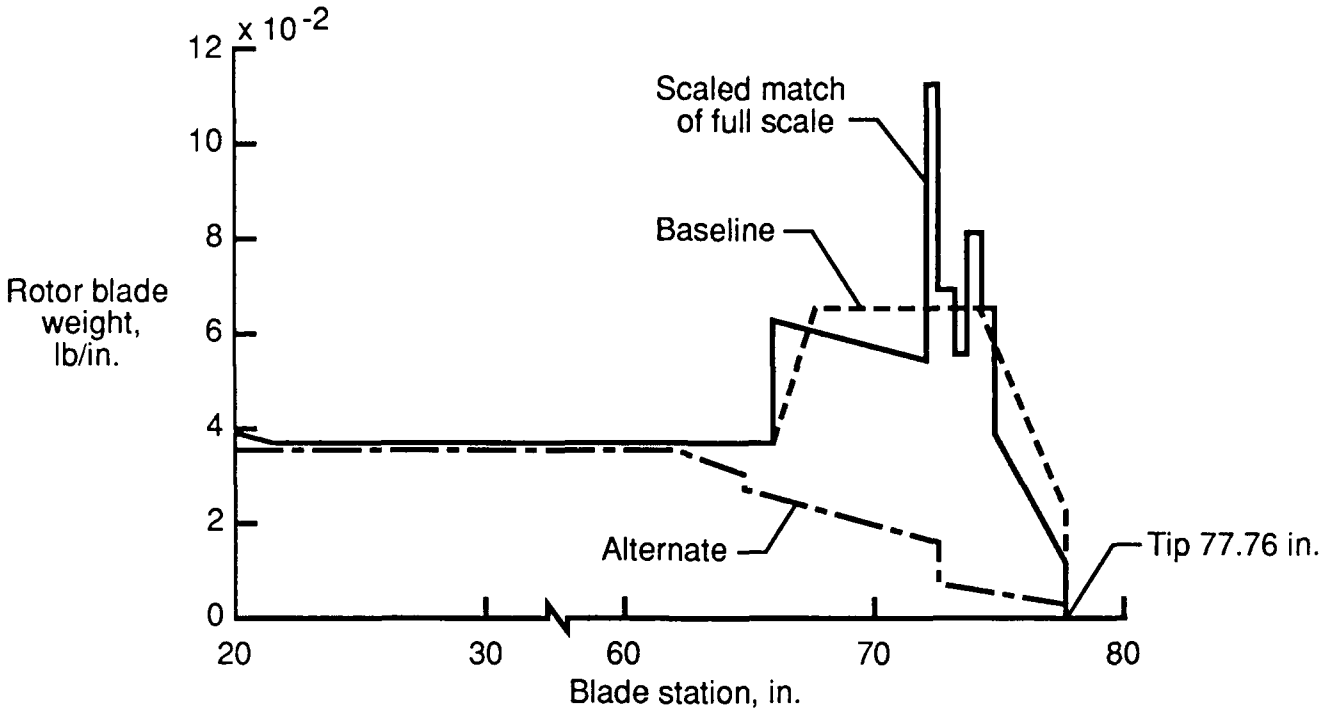

Figure 7. Rotor blade weight as a function of blade radial station.

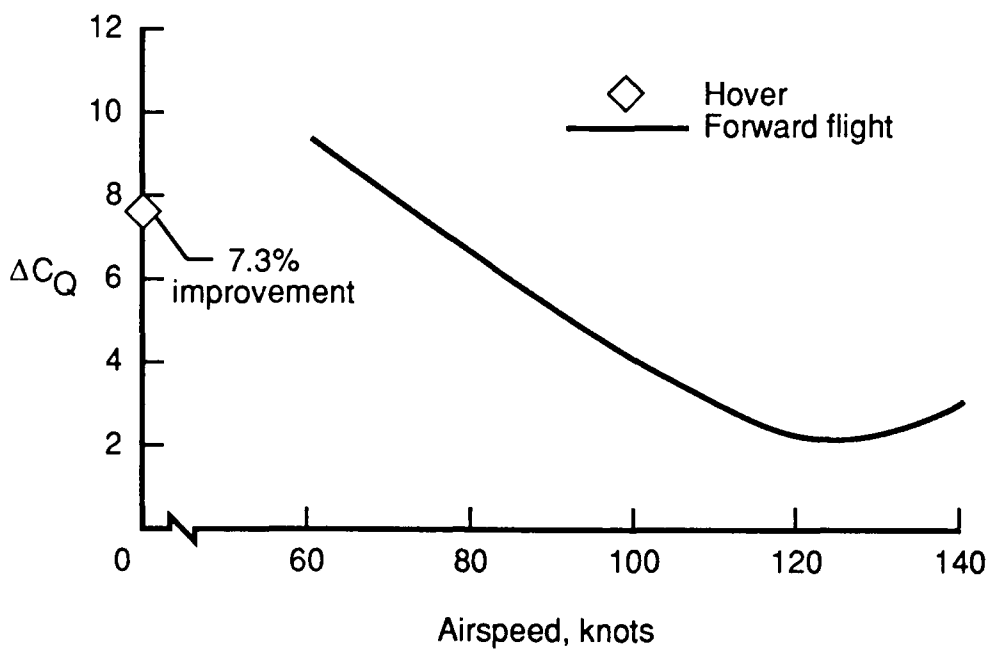

Figure 8. Analytical prediction of performance improvement of alternate rotor compared with baseline rotor. SLS atmospheric conditions; $f = 33.8$ ft^2; $C_T = 0.0064$.

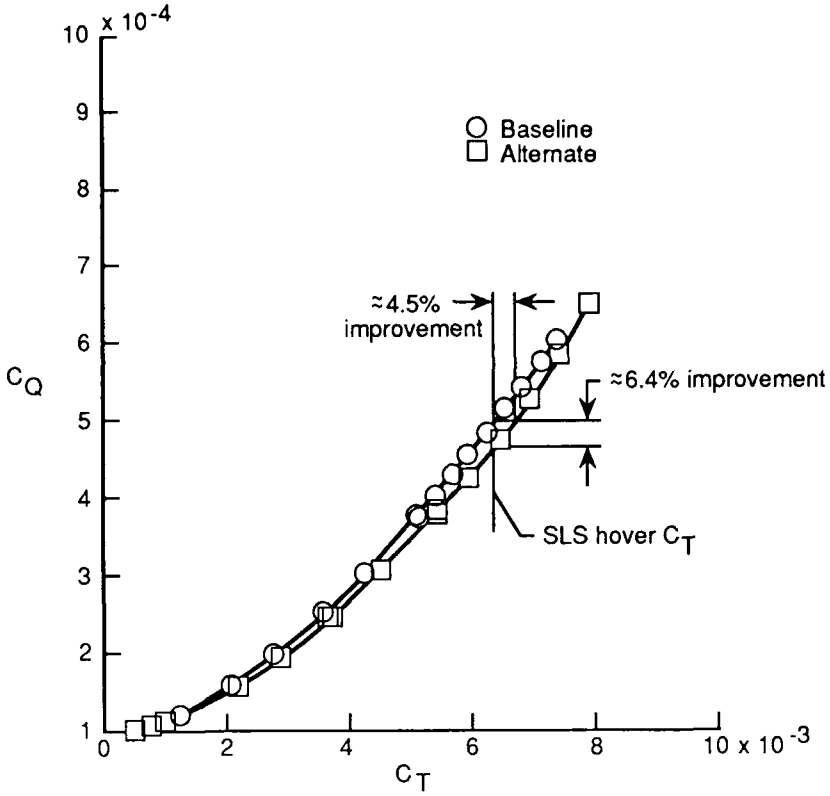

Figure 9. Rotor torque coefficient versus thrust coefficient for baseline and alternate rotors in hover at $M_{tip} = 0.64$ and $H/d = 1.4$.

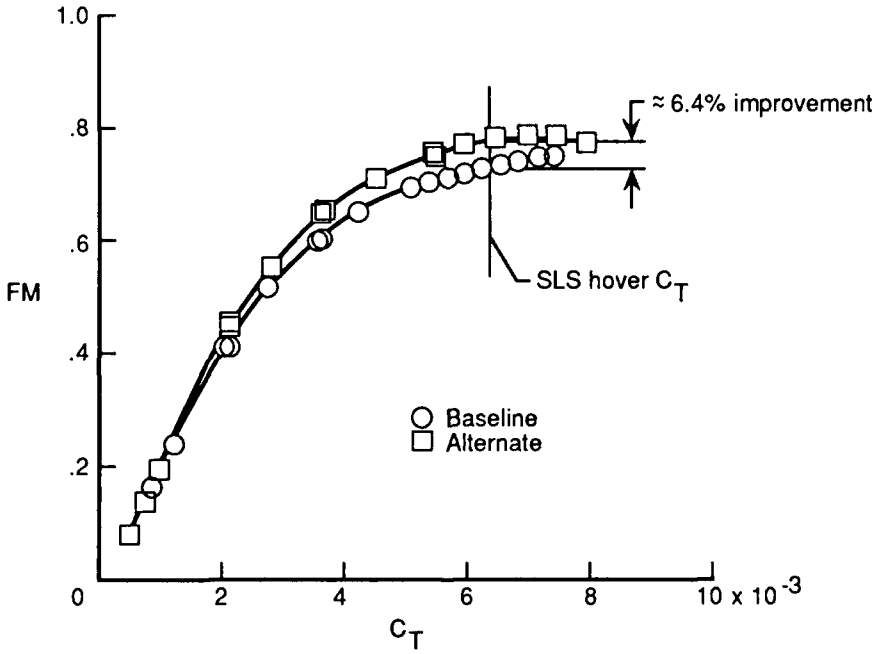

Figure 10. Rotor figure of merit versus thrust coefficient for baseline and alternate rotors in hover at $M_{tip} = 0.64$ and $H/d = 1.4$.

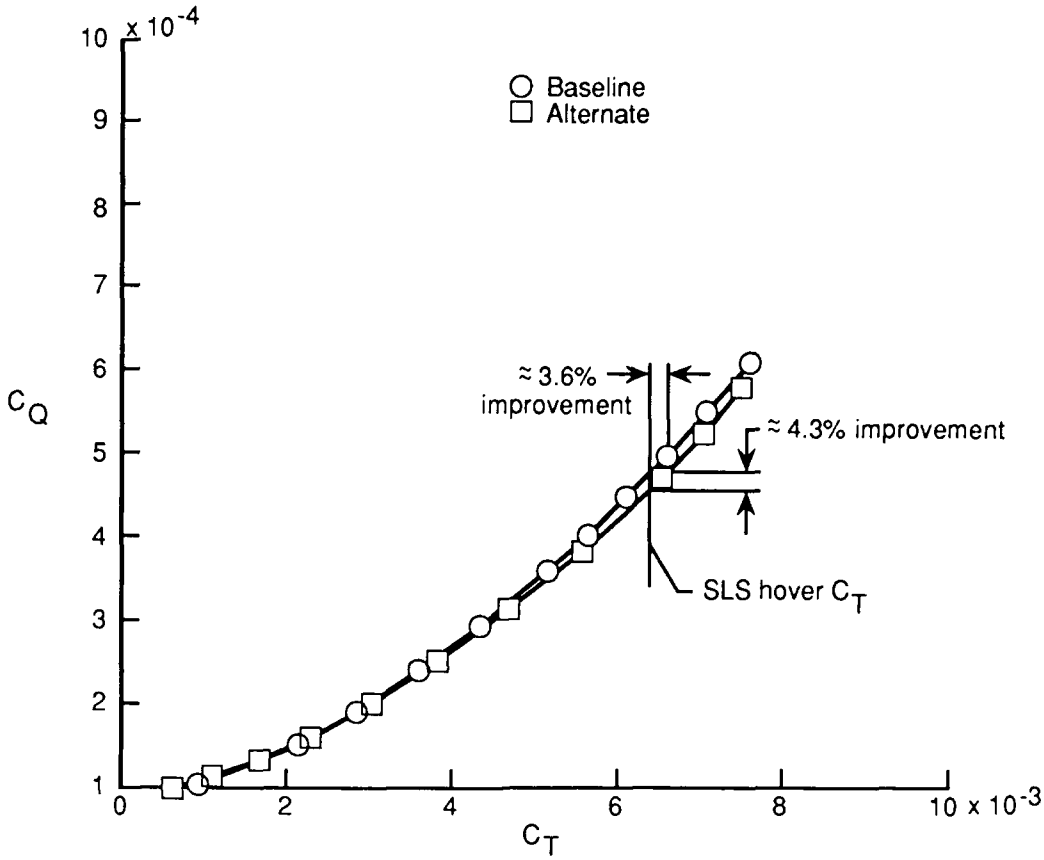

Figure 11. Rotor torque coefficient versus thrust coefficient for baseline and alternate rotors in hover at $M_{\text{tip}} = 0.58$ and $H/d = 1.4$.

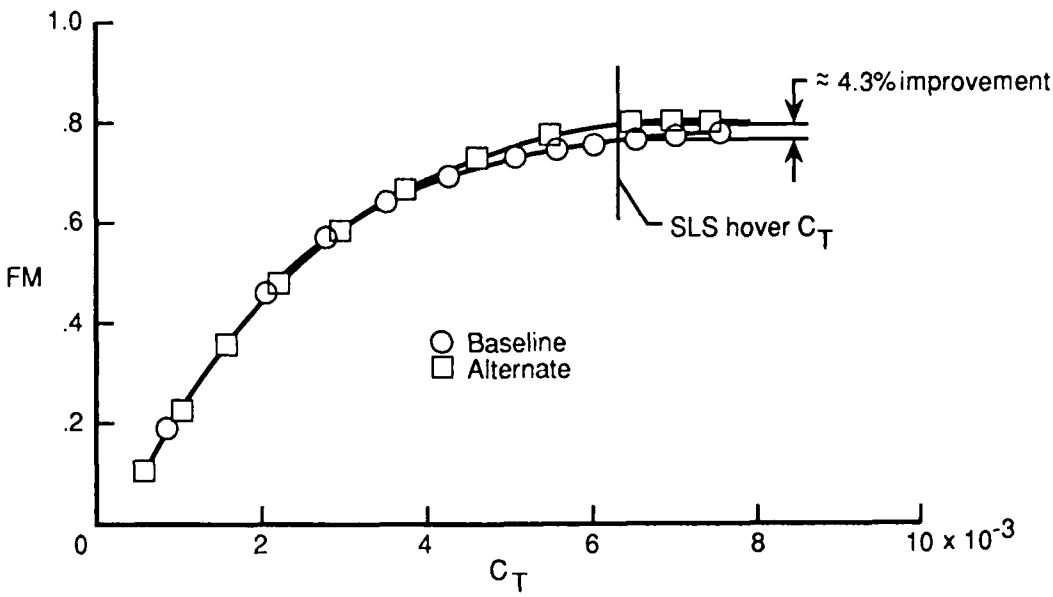

Figure 12. Rotor figure of merit versus thrust coefficient for baseline and alternate rotors in hover at $M_{\text{tip}} = 0.58$ and $H/d = 1.4$.

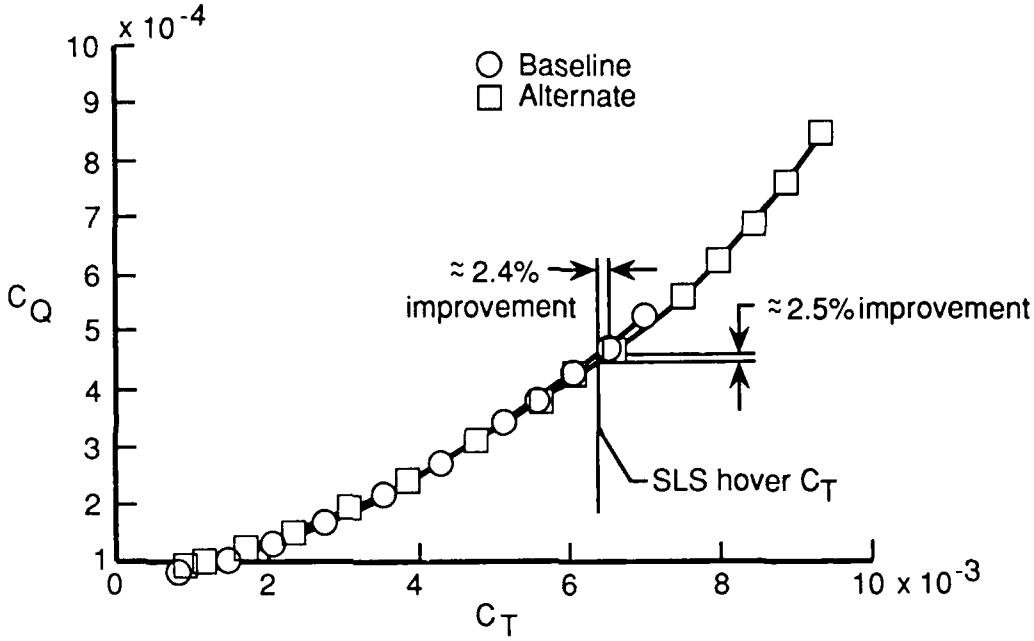

Figure 13. Rotor torque coefficient versus rotor thrust coefficient for baseline and alternate rotors in hover at $M_{tip} = 0.51$ and $H/d = 1.4$.

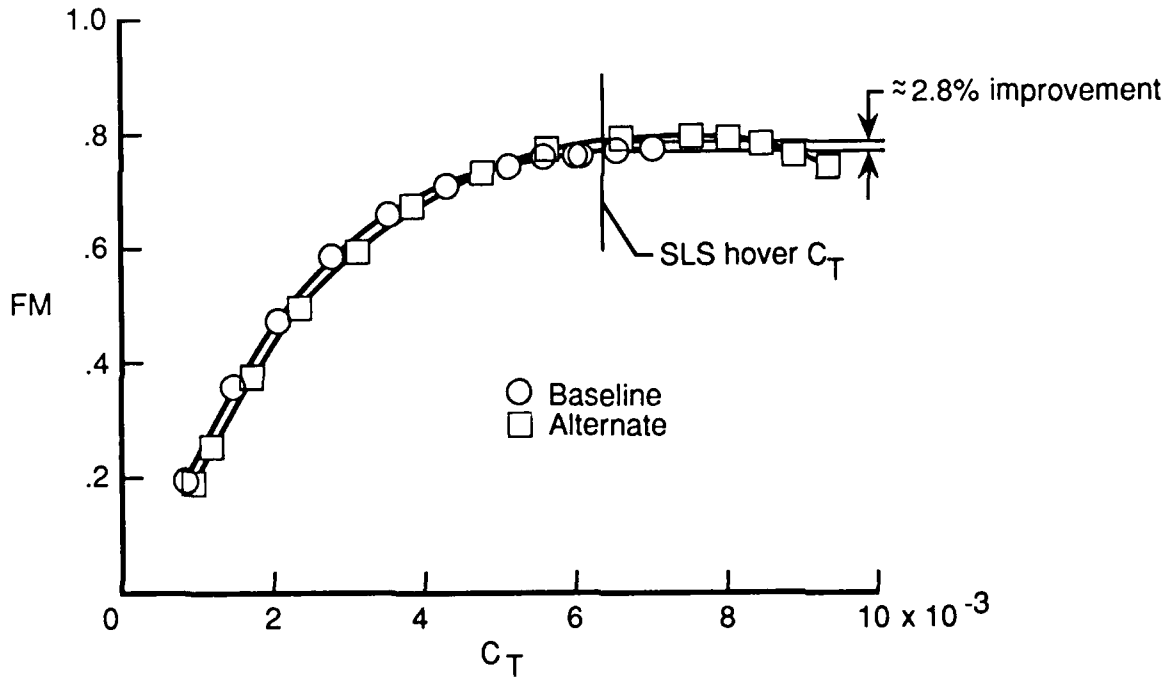

Figure 14. Rotor figure of merit versus rotor thrust coefficient for baseline and alternate rotors in hover at $M_{tip} = 0.51$ and $H/d = 1.4$.

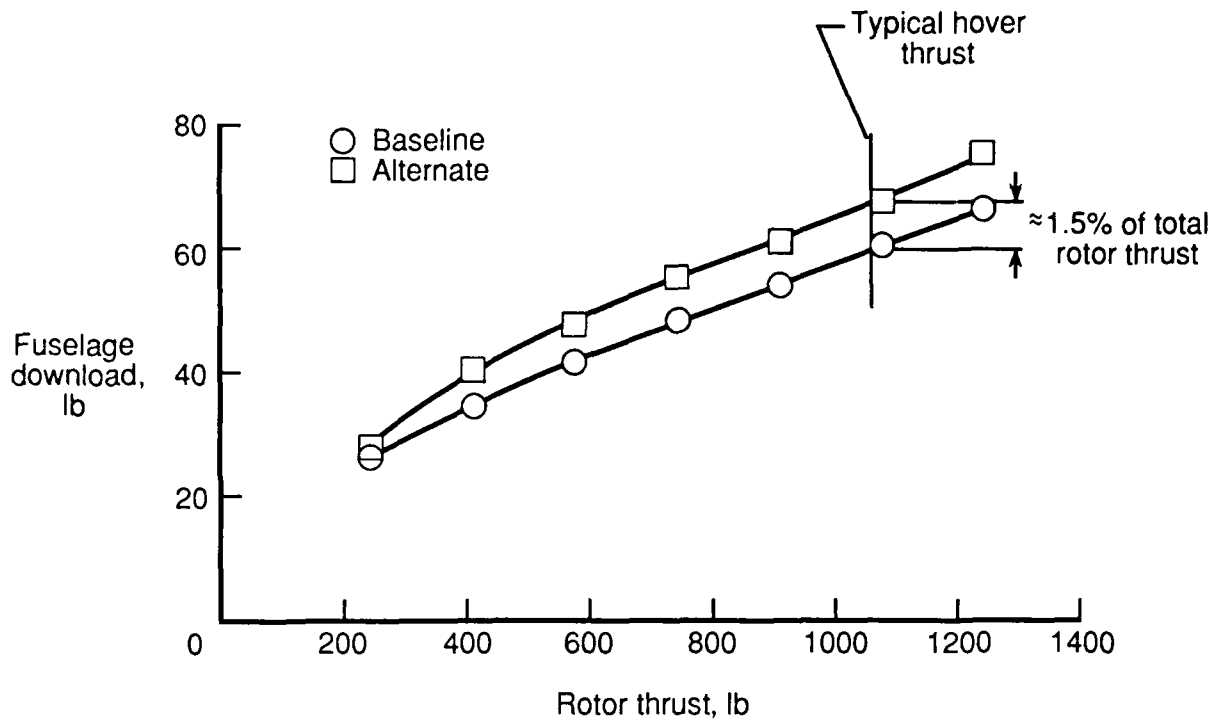

Figure 15. Fuselage download versus rotor thrust for baseline and alternate rotors in hover at $M_{tip} = 0.64$ and $H/d = 1.4$.

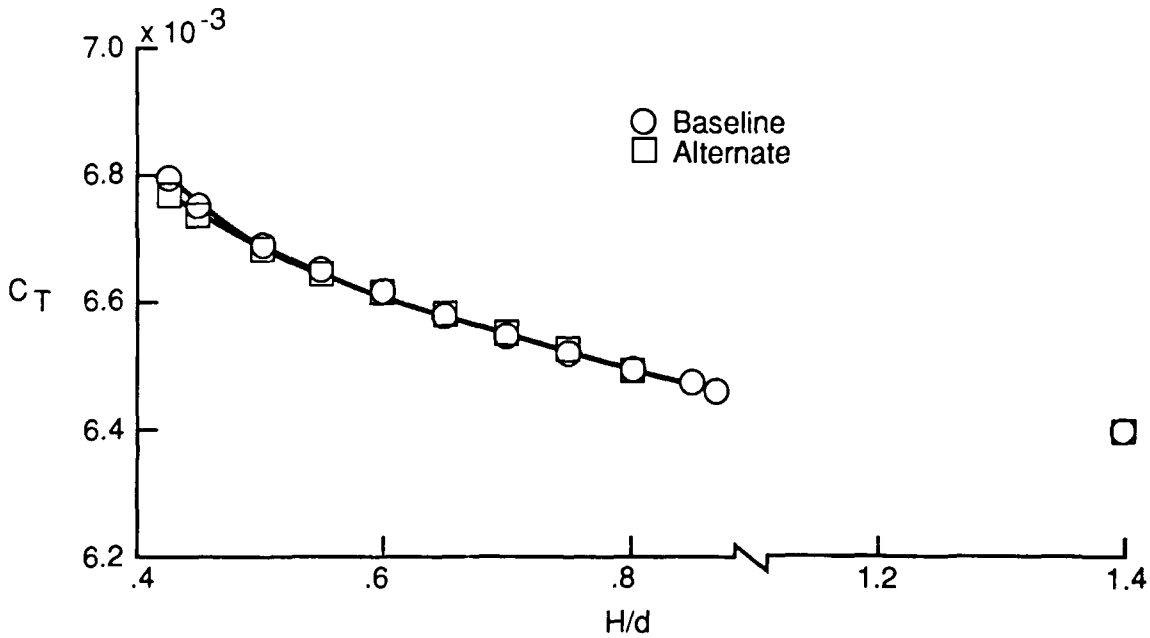

Figure 16. Effect of ground proximity on rotor thrust coefficient for baseline and alternate rotors in hover at $M_{tip} = 0.64$ and $C_Q = 0.00048$.

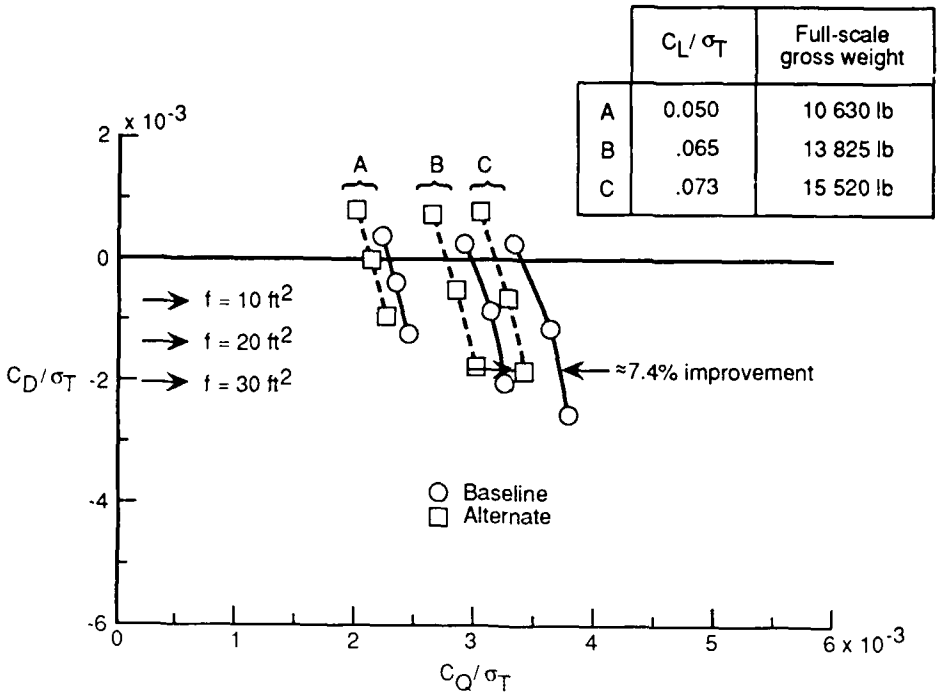

(a) $\mu = 0.15$.

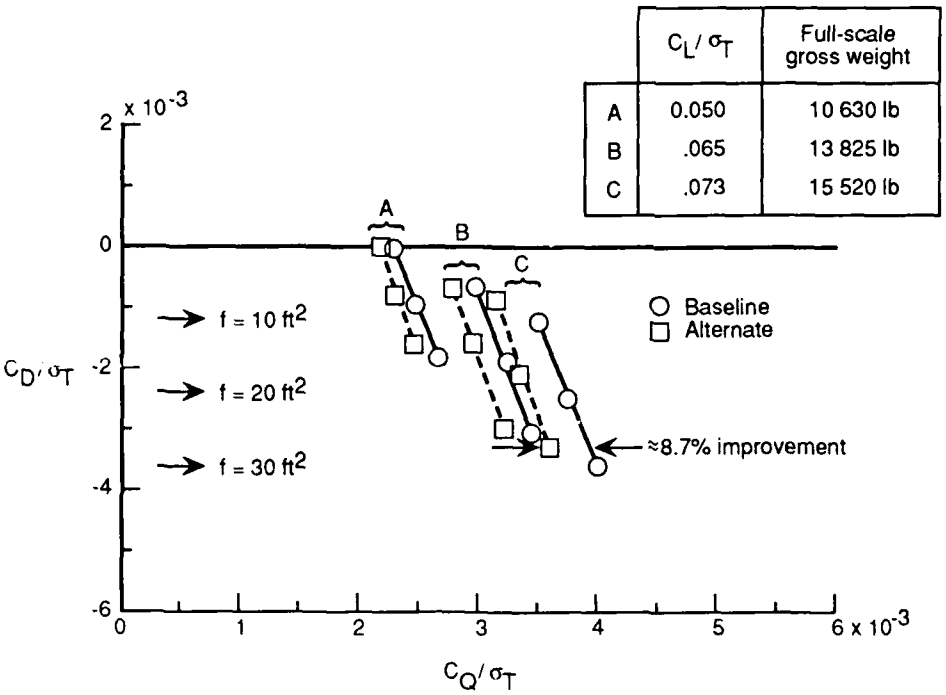

(b) $\mu = 0.20$.

Figure 17. Rotor drag coefficient versus rotor torque coefficient at three values of rotor lift for baseline and alternate rotors in forward flight.

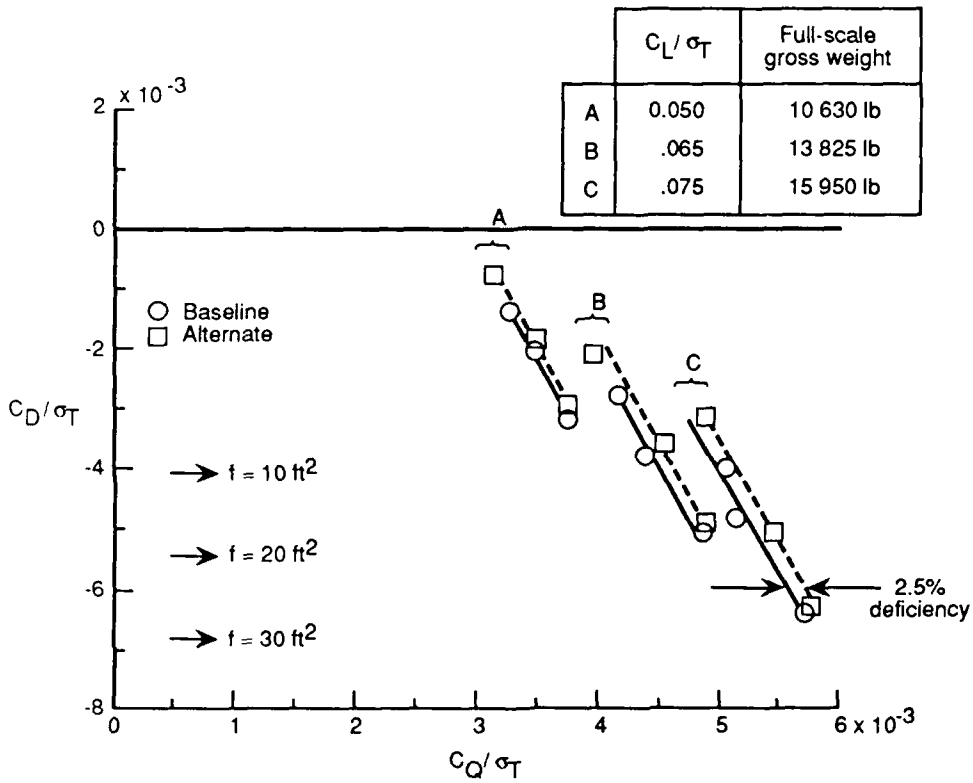

(c) $\mu = 0.30$.

Figure 17. Concluded.

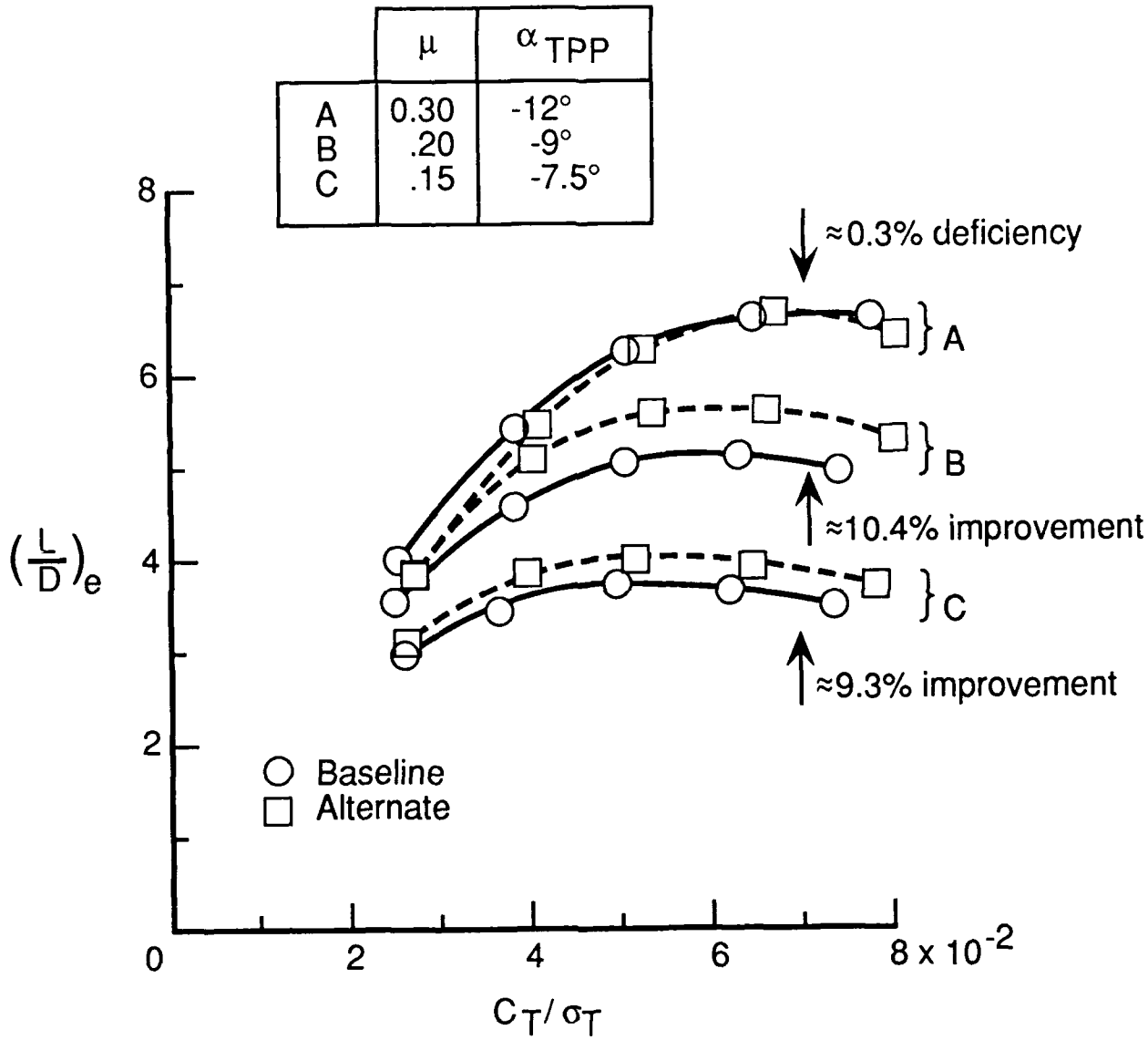

Figure 18. Rotor lift drag ratio versus rotor thrust coefficient at three advance ratios for baseline and alternate rotors (hub drag removed from calculations.)

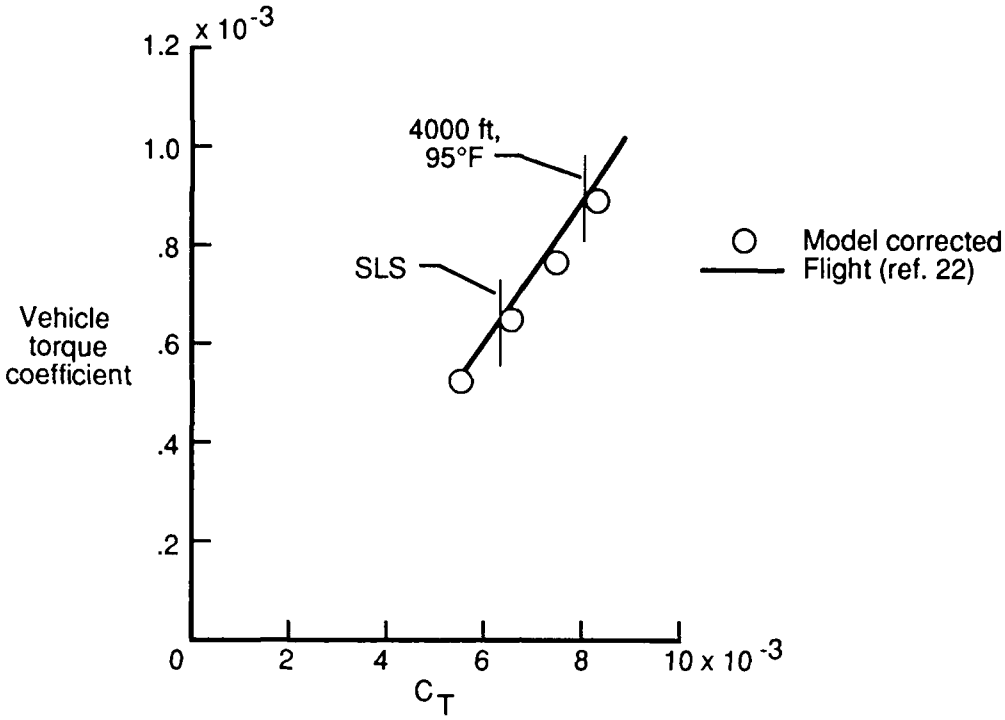

Figure 19. Comparison of baseline AH-64 model rotor performance with flight-test results in hover. $M_{\text{tip}} = 0.64$; hover OGE.

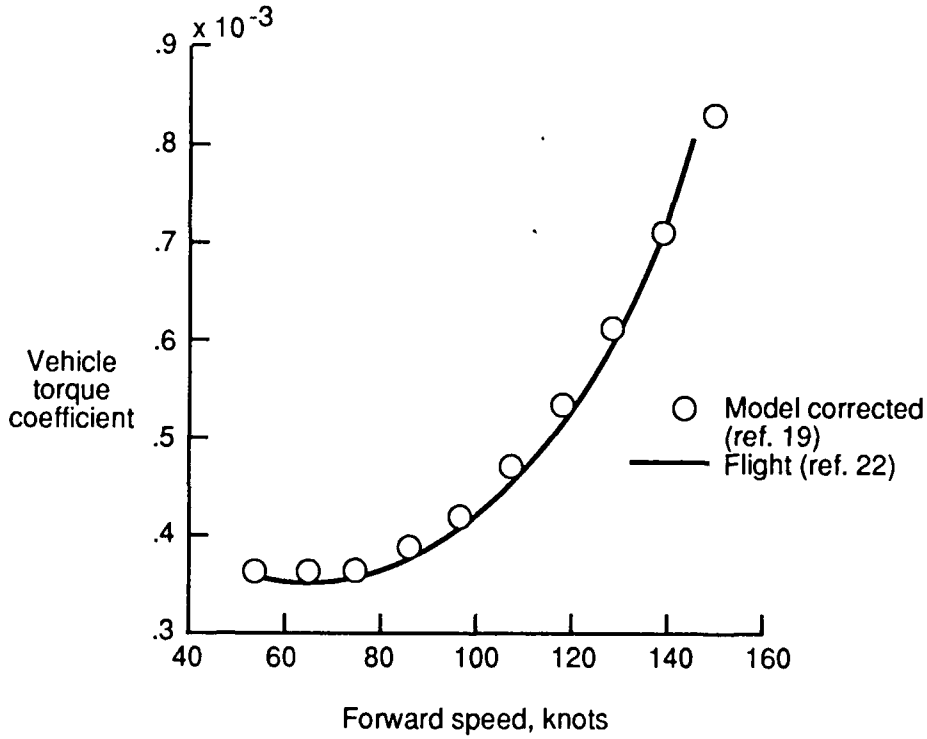

Figure 20. Comparison of baseline AH-64 model performance with flight-test results in forward flight. $C_T = 0.0064$; $f = 33.8$ ft^2; SLS atmospheric conditions.

NASA

Report Documentation Page

1. Report No. NASA TM-4201 AVSCOM TM-90-B-015	2. Government Accession No.	3. Recipient's Catalog No
4. Title and Subtitle Aerodynamic Performance of a 0.27-Scale Model of an AH-64 With Baseline and Alternate Rotor Blade Sets		5. Report Date July 1990
		6. Performing Organization Code
7. Author(s) Henry L. Kelley		8. Performing Organization Report No. L-16725
9. Performing Organization Name and Address Aerostructures Directorate USAARTA-AVSCOM Langley Research Center Hampton, VA 23665-5225		10. Work Unit No. 505-61-51-10
		11. Contract or Grant No.
12. Sponsoring Agency Name and Address National Aeronautics and Space Administration Washington, DC 20546-0001 and U.S. Army Aviation Systems Command St. Louis, MO 63120-1798		13. Type of Report and Period Covered Technical Memorandum
		14. Army Project No. 1L162211AH7AA

15. Supplementary Notes

Henry L. Kelley: Aerostructures Directorate, USAARTA-AVSCOM.

16. Abstract

Performance of a 0.27-scale rotor model designed for the AH-64 Apache helicopter (alternate rotor) was measured in hover and forward flight and compared with an AH-64 baseline rotor model. Thrust, rotor tip Mach number, advance ratio, and ground proximity were varied. In hover, at a nominal thrust coefficient of 0.0064, the alternate rotor used about 6.4 percent less power than the baseline rotor. The corresponding thrust increase at this representative hover power condition was approximately 4.5 percent, which represents an equivalent full-scale increase in lift capability of about 660 lb. Comparable results were noted in forward flight, except for the high-thrust, high-speed cases investigated (Advance ratio = 0.30), where the baseline rotor was slightly superior. Reduced performance at the higher thrusts and speeds was probably caused by Reynolds number effects and blade elasticity differences.

17. Key Words (Suggested by Authors(s)) Helicopters Rotor performance Model rotor testing Tapered rotor blades Ground effects		18. Distribution Statement Unclassified—Unlimited Subject Category 02	
19. Security Classif. (of this report) Unclassified	20. Security Classif. (of this page) Unclassified	21. No. of Pages 22	22. Price A03

NASA FORM 1626 OCT 86 NASA-Langley, 1990

For sale by the National Technical Information Service, Springfield, Virginia 22161-2171